Adaptive frequency-domain block correlators for range processing in digital automotive radars

Hanqing Wu
NXP Semiconductors
Eindhoven, The Netherlands
hanqing.wu@nxp.com

Geert Leus
Delft University of Technology
Delft, The Netherlands
g.j.t.leus@tudelft.nl

Ashish Pandharipande
NXP Semiconductors
Eindhoven, The Netherlands
ashish.pandharipande@nxp.com

***Abstract*—The use of digital sequences in automotive radars provides better support for multiple antennas in imaging radar applications. However, a challenge in such digital radars is the higher complexity in the receiver processing chain, starting from the bank of correlators used to estimate the range of targets. State-of-the-art correlators are implemented using using fast Fourier transforms (FFTs), which have log linear complexity in the FFT length used in correlating the digital sequence with the received sequence. This results in high complexity due to the large sequence lengths needed to achieve high sensing range and fine velocity resolution. We propose an adaptive block FFT-based correlator processing method that exploits sparsity in the range domain. In comparison to conventional FFT-based correlator processing, the proposed method provides a significant reduction in complexity.**

***Index Terms*—Frequency-domain correlator, range processing, digital radar.**

I. Introduction

Automotive radars play a critical role in providing robust scene understanding in an advanced driver assistance system (ADAS) to improve driving comfort and road safety while enabling higher levels of automation. Multiple input multiple output (MIMO) imaging radar is essential for achieving high-resolution measurements of target range, speed, and angular position [1], [2]. However, conventional analog frequency modulated continuous wave (FMCW) radars face MIMO scaling limitations due to high Doppler velocity ambiguities. The use of orthogonal digital waveforms has therefore attracted attention [3]–[6]. An example of such radars is a phase modulated continuous wave (PMCW) radar that uses orthogonal binary codes and advanced signal processing [7]–[9].

A binary PMCW radar, shown in Fig. 1, transmits a continuous RF carrier modulated by binary sequences with levels {-1, +1}, representing 0° or 180° phase shifts. High-performance modulation relies on sequences with favorable auto-correlation and cross-correlation properties, a large set size, and longer code lengths to support MIMO and improve target discrimination. To achieve high unambiguous detection range and fine velocity resolution, a long sequence length is required. Commonly used sequences include almost perfect auto-correlation sequences (APAS), zero correlation zone sequences, and Gold codes [10]–[12], which modulate a 79 GHz local oscillator (LO). The received signal, delayed and scaled by range, undergoes amplification, down-conversion, digitization, and then range and Doppler processing.

This work was supported in part by the Dutch Ministry of Economic Affairs and Climate Policy and in part by the Important Projects of Common European Interest (IPCEI) Microelectronics and Communication Technology (ME/CT) Project.

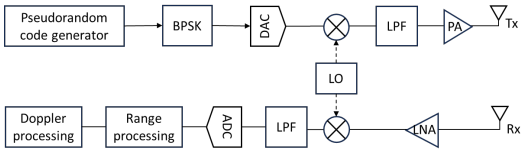

Fig. 1: Illustrative single antenna PMCW radar.

Range processing in PMCW radars is done using a correlator bank to estimate signal delays reflected from targets. Correlators can operate in the time domain [13]–[16], with simple hardware at the cost of higher computational demand, or in the frequency domain [17], [18], where fast Fourier transforms (FFTs) enable efficient parallel processing especially for large values of L_c. Real-time radar applications demand reduced correlation complexity with lower power consumption. We address the problem of reducing the complexity of such frequency-domain correlators.

Digital correlators are also used in other applications like wireless ranging and global navigation satellite system (GNSS) acquisition, and the problem of correlator design with reduced complexity has been considered in the past. Studies have focused on fast algorithms to reduce the complexity of time-domain correlators [14]–[16]. In the frequency domain, block FFT splitting based correlators [17], [19] were proposed based on the well-known block FFT Cooley-Tuckey implementation [20] to lower the memory resource use and processing complexity of GNSS signal acquisition. The correlation architecture involves splitting FFTs into smaller, fixed block FFTs spanning the full range. This however limits the flexibility and scalability of such a solution for PMCW radars, and fails to exploit the sparsity inherent in automotive radar signals.

In this paper, we exploit the inherent sparsity in the radar received signals. Building on the full block correlator in [19], the adaptive FFT-based block correlator with Doppler processing proposed in our paper reduces complexity by dynamically identifying and processing only the relevant range profile blocks, where potential targets are present. Simulation results demonstrate that the proposed block correlator maintains target

detections while achieving superior computational efficiency compared to a traditional FFT-based correlator.

II. Frequency Domain Correlator

In a PMCW radar system with a code $c[n]$ of length L_c and symbol duration T_c, range processing is performed using correlator banks that compare the received signal $y[n]$ with delayed versions of $c[n]$ at τT_c. The resulting range profile exhibits peaks at time-of-flight reflections, enabling distance estimation. Since time-domain correlation corresponds to element-wise multiplication in the frequency domain, the range profile $r[\tau]$ can be computed using the FFT, element-wise multiplication, and inverse FFT, as shown in Fig. 2. As the lengths L_c of commonly used sequences such as APAS and Gold codes are generally not powers of two, both the code $c[n]$ and the received signal $y[n]$ are zero-padded to the nearest power-of-two length L to enable efficient FFT implementation.

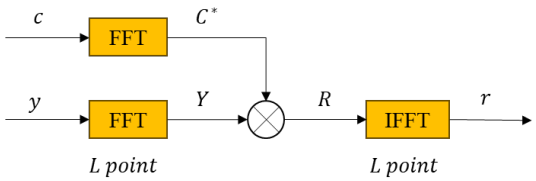

Fig. 2: Block diagram of a frequency-domain correlator.

The FFT-transformed received and transmitted signals are respectively

$$Y[k] = \sum_{n=0}^{L-1} y[n] e^{-j\frac{2\pi}{L}kn}, \quad C[k] = \sum_{n=0}^{L-1} c[n] e^{-j\frac{2\pi}{L}kn}. \quad (1)$$

The frequency-domain correlation is then obtained as

$$R[k] = Y[k]C^*[k] = \sum_{\tau=0}^{L-1} \underbrace{\sum_{n=0}^{L-1} y[n]c[(n-\tau) \bmod L]}_{r[\tau]} e^{-j\frac{2\pi}{L}k\tau}. \quad (2)$$

A subsequent IFFT results in the time-domain range profile

$$r[\tau] = \frac{1}{L} \sum_{k=0}^{L-1} R[k] e^{j\frac{2\pi}{L}k\tau}. \quad (3)$$

Although this frequency-domain approach has a reduced complexity of $\mathcal{O}(L \log L)$ compared to time-domain correlators, it remains computationally demanding for large L_c, motivating the need for lower complexity approaches.

III. Adaptive FFT-based block correlator

In automotive radar scenarios, only a limited number of targets exist within the radar's field of view. Furthermore, in ADAS applications, the nearby targets are more relevant for actions like braking and cruise control. Consequently, radar signals exhibit inherent sparsity, with many range bins containing minimal or no relevant target information, and only a small subset of detections being relevant.

Leveraging range sparsity, we propose an adaptive FFT-based block correlator by dynamically identifying and processing only the relevant range profile blocks where potential targets are likely to be present. While primarily designed for range processing, it operates within a broader radar framework that includes Doppler processing, as illustrated in Fig. 3. The figure depicts a single frame consisting of M fast-time durations. Range processing is performed within each fast-time duration, while Doppler processing analyzes phase shifts across pulses to estimate target velocities. The figure provides an overview of this integrated processing pipeline, and the key processing steps are now outlined.

A. Initial Range Processing

During the initial fast-time duration of the radar frame, a full block correlator generates a preliminary range profile. This correlator implementation, shown in Fig. 4 is based on segmenting the whole sequence into d smaller blocks. We first note that the full block correlator in Fig. 4 is equivalent to the frequency domain correlator in Fig. 2, [17], [19]. We then describe the involved processing steps, based on which the proposed adaptive structure of Fig. 3 builds on.

1) Padding and segmentation: The received $y[n]$ is first zero-padded to a length L that is a multiple of d and a power of 2, and then segmented into d blocks $y_i[n]$ where:

$$y_i[n] = y[n + (i-1)L/d], \quad n \in \{0, 1, \cdots, L/d - 1\}. \quad (4)$$

The transmitted code sequence $c[n]$ is similarly padded, segmented and could be precomputed for storage.

2) Combination: In the combination block, each segment $y_i[n]$ is processed using phase shifts as follows:

$$\tilde{y}_m[n] = \left(\sum_{i=1}^{d} y_i[n] e^{\frac{-j2\pi(m-1)(i-1)}{d}} \right) e^{\frac{-j2\pi(m-1)n}{L}}. \quad (5)$$

3) L/d-point FFTs: A L/d-point FFT is applied to $\tilde{y}_m[n]$ for each m, yielding:

$$\tilde{Y}_m[k] = \sum_{n=0}^{L/d-1} \tilde{y}_m[n] e^{\frac{-j2\pi kn}{L/d}}, \quad k \in \{0, \cdots, L/d - 1\}. \quad (6)$$

$\tilde{Y}_m[k]$ can be seen as a down-sampled version of the original $Y[k]$ by a factor d, expressed as $\tilde{Y}_m[k] = Y[dk + m - 1]$. The relationship follows directly from the expression of $Y[k]$ in terms of its segmented parts.

$$Y[k] = \sum_{n=0}^{L/d-1} \left(\sum_{i=1}^{d} y_i[n] e^{-\frac{j2\pi k(i-1)}{d}} \right) e^{-\frac{j2\pi kn}{L}}. \quad (7)$$

4) Multiplication in the frequency domain: For each segment ($m = 1, 2, \ldots, d$), element-wise multiplication is performed between $\tilde{Y}_m[k]$ and the conjugate of $\tilde{C}_m[k]$, yielding:

$$\tilde{R}_m[k] = \tilde{Y}_m[k] \tilde{C}^*_m[k]. \quad (8)$$

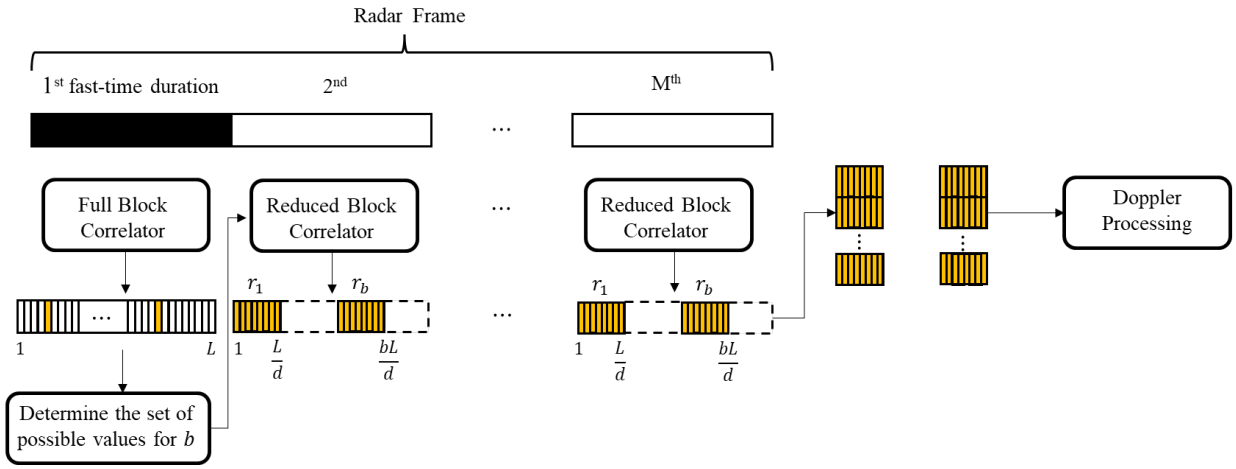

Fig. 3: Architecture of the adaptive FFT-based block correlator with Doppler processing. Adaptation occurs across different frames, while each frame involves a reduced size of FFT blocks in the correlator.

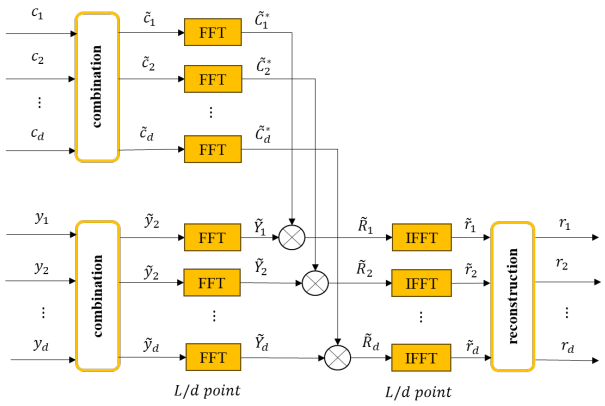

Fig. 4: Structure of block FFT-based correlator.

By substituting $\tilde{Y}_m[k]$ and $\tilde{C}_m[k]$, the down-sampling relationship between $\tilde{R}_m$ and R is established as follows:

$$\begin{aligned}\tilde{R}_m[k] &= R[dk+m-1] \qquad (9)\\ &= \sum_{\tau=0}^{L/d-1}\left(\sum_{i=1}^{d} r_i[\tau] e^{\frac{-j2\pi(dk+m-1)(i-1)}{d}}\right) e^{\frac{-j2\pi(dk+m-1)\tau}{L}}\\ &= \sum_{\tau=0}^{L/d-1}\underbrace{\left(\sum_{i=1}^{d} r_i[\tau] e^{\frac{-j2\pi(m-1)(i-1)}{d}}\right) e^{\frac{-j2\pi(m-1)\tau}{L}}}_{\tilde{r}_m[\tau]} e^{\frac{-j2\pi k\tau}{L/d}}\end{aligned}$$

where $r_i[\tau] = r[\tau + (i-1)L/d]$ represents the i_{th} segmented range profile.

5) L/d-point IFFTs: The IFFT is applied to compute $\tilde{r}_m[\tau]$ for each m, where $\tau \in \{0, \ldots, L/d-1\}$, given by:

$$\tilde{r}_m[\tau] = \frac{1}{L/d}\sum_{k=0}^{L/d-1} \tilde{R}_m[k] e^{\frac{j2\pi k\tau}{L/d}}. \qquad (10)$$

6) Reconstruction: Each block range profile $\hat{r}_b$ for $b \in \{1, 2, \cdots, d\}$ could be reconstructed independently by combining the segmented components $\tilde{r}_m[\tau]$ as follows:

$$\begin{aligned}\hat{r}_b[\tau] &= \frac{1}{d}\sum_{m=1}^{d} \tilde{r}_m[\tau] e^{\frac{j2\pi(m-1)\tau}{L}} e^{\frac{j2\pi(b-1)(m-1)}{d}} \qquad (11)\\ &= \frac{1}{d}\sum_{i=1}^{d} r_i[\tau]\left(\sum_{m=1}^{d} e^{\frac{-j2\pi(m-1)(i-b)}{d}}\right) = r_b[\tau].\end{aligned}$$

Thus the full block correlator gives the same range profile as the frequency-domain correlator in Fig. 2.

B. Range Bin Selection for Efficient Processing

The initial range profile is analyzed using a noise power-dependent threshold detector, such as the constant false alarm rate (CFAR) algorithm, to identify range bins with potential targets, highlighted in orange in Figure 3. Once potential targets are detected, the algorithm determines the set of possible values for b, where b represents the blocks containing relevant range bins where targets are present. For example, with a total range of $L = 1024$ bins divided into $d = 4$ equal blocks of 256 bins each, the targets at bins 150 and 700 fall into blocks $[1, 256]$ and $[513, 768]$, respectively. As a result, the algorithm selects blocks $b = 1$ and $b = 3$ for further processing.

C. Reduced FFT-based block correlator

Once the selection of range bin blocks is done, for the remaining $M-1$ slow-time durations in one frame, a reduced block correlator is employed. Given d blocks and the identified set of possible values for b, the reduced block correlator reconstructs only the relevant block range profiles $\hat{r}_b$ by combining the segmented components $\tilde{r}_m[\tau]$ as given in (11).

D. Frame-by-frame adaptation

After one frame, Doppler processing is applied to each relevant block $\hat{r}_b$ across all M fast-time durations using M-point FFTs. Instead of covering the full range which requires

L instances of M-point FFTs, the reduced correlator focuses only on regions with potential targets. This reduces the computational burden to L/d instances of M-point FFTs when processing a single block, significantly improving efficiency. Complexity analysis will be discussed in the following section.

At the start of each new frame, the system re-evaluates the full range bins to account for changes in the target environment. Since the range bins of interest are updated every measurement period (typically, 20–30 ms), target movement within this duration is small. Consequently, detected targets are likely to remain within the adjacent bins in the same block, ensuring consistent tracking and detection. By dynamically adapting the selection of relevant blocks for both range and Doppler processing on a frame-by-frame basis, the proposed approach effectively reduces computational complexity while maintaining reliable performance.

IV. Performance Evaluation

We evaluate the performance of the adaptive FFT-based block correlator in comparison to the conventional frequency-domain correlator, focusing on both range and Doppler processing. Since the complexity of Doppler processing is directly influenced by correlation results, as discussed in Section III-D, it is also incorporated into the analysis.

A. Complexity Analysis

Consider a MIMO configuration with $N_{\mathrm{T}} \times N_{\mathrm{R}}$ antennas and a slow-time size M. The well-known computational complexity of an N-point FFT [20] requires $\frac{N}{2}\log N$ complex multiplications and $N \log N$ complex additions. Each complex multiplication involves 4 real multiplications and 2 real additions, while a complex addition involves 2 real additions.

1) Complexity of applying FFT-based correlator: As shown in Figure 2, range processing involves two L-point FFTs and one L-point IFFT. Since the FFT of the transmitted codes can be precomputed and stored, the computational complexity is determined by three main operations: computing $Y[k]$, performing multiplication in the frequency domain, and applying the IFFT. For Doppler processing in a single antenna system, we need L times an M-point FFT. In a MIMO radar configuration, the computational complexity for both range and Doppler processing is detailed in Table I.

2) Complexity of the adaptive FFT-based block correlator: According to (5), the combination step requires dL complex multiplications and additions, along with an additional $(d-1)L/d$ complex multiplications for phase adjustments, which simplifies to L. The d block FFTs, each of length L/d, require $2L\log_2 L/d$ real multiplications and $3L\log_2 L/d$ real additions. For the MIMO configuration, the total complexity is scaled by a factor of $N_{\mathrm{R}}M$. The multiplication in the frequency domain requires $N_{\mathrm{T}}N_{\mathrm{R}}ML$ complex multiplications. For the IFFT stage, the d IFFTs of length L/d require $2N_{\mathrm{T}}N_{\mathrm{R}}ML\log_2 L/d$ real multiplications and $3N_{\mathrm{T}}N_{\mathrm{R}}ML_c\log_2 L/d$ real additions. The final reconstruction step, as described in (11), involves $(d-1)$ L/d-length complex multiplications and additions, which are approximated as L. For Doppler processing, we only need L/d times an M-point FFT. The complexity for applying the proposed correlator is provided in Table I.

3) Complexity comparison: We now assess the computational complexity of the fixed and adaptive correlators in terms of operations shown in Tables I. For evaluation, we consider a 4×4 MIMO configuration and slow time size of $M = 2048$. The complexity is analyzed using a Gold sequence of length 2047. Since FFT operations require zero-padding to the nearest power of two, we set $L = 2048$.

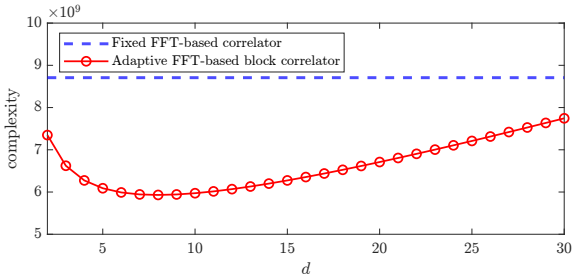

Fig. 5: Complexity comparison of range and Doppler processing in terms of total # MUL and # ADD operations for a Gold sequence.

As shown in Fig. 5, the adaptive block correlator exhibits lower computational complexity in comparison to the frequency-domain correlator for different d. The most significant reduction occurs at $d = 8$, where it achieves approximately a 32% decrease in complexity compared to the conventional frequency-domain correlator.

B. Simulation Result

Simulations were conducted with optimal parameter $d = 8$, considering two targets: one car with an RCS of 10 dBsm at 50 m and 10°, moving at 20 m/s, and a truck with an RCS of 25 dBsm, positioned at 100 m and -5°, moving at 30 m/s.

From initial range processing, targets are located in the second and third blocks, requiring the reconstruction of $\hat{r}_2$ and $\hat{r}_3$. As shown in Fig. 6, the range-Doppler map (RDM) comparison indicates that the proposed approach preserves the target peak and maintains the same noise floor as the conventional frequency domain approach, ensuring an equivalent signal-to-noise ratio (SNR) and thus target detection performance. Simulations show a reduction in computation time from 8.91 to 5.16 seconds, achieving significant speedup without compromising detection accuracy. While this evaluation is based on MATLAB simulations and does not account for hardware processing, the reduction in processing time is indicative of the achievable gains.

V. Conclusions

We presented an adaptive FFT-based block correlator for digital automotive radar. By selectively processing only the range bins of interest, this approach significantly reduces computational complexity while maintaining target detections. Simulations confirmed its effectiveness, showing that target

TABLE I: Complexity Comparison: FFT-based vs. adaptive FFT-based block correlator

Operation	FFT-based Correlator	Adaptive FFT-based Block Correlator
Range Processing		
# MUL	$2(N_R + N_T N_R)ML \log_2 L + 4N_T N_R ML$	$2(N_R + N_T N_R)ML \log_2 \frac{L}{d} + (8N_T + 4d + 4)N_R ML$
# ADD	$3(N_R + N_T N_R)ML \log_2 L + 2N_T N_R ML$	$3(N_R + N_T N_R)ML \log_2 \frac{L}{d} + (6N_T + 4d + 2)N_R ML$
Doppler Processing		
# MUL	$2N_T N_R ML \log_2 M$	$2N_T N_R M \frac{L}{d} \log_2 M$
# ADD	$3N_T N_R ML \log_2 M$	$3N_T N_R M \frac{L}{d} \log_2 M$

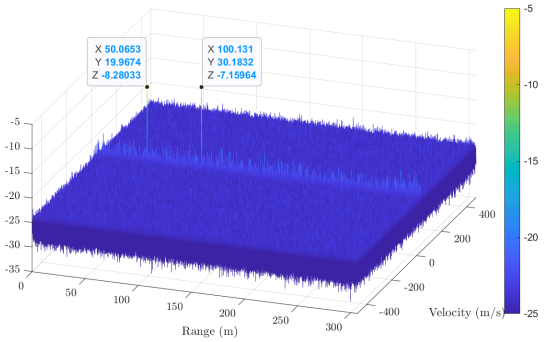

(a) RDM with full FFT-based correlator.

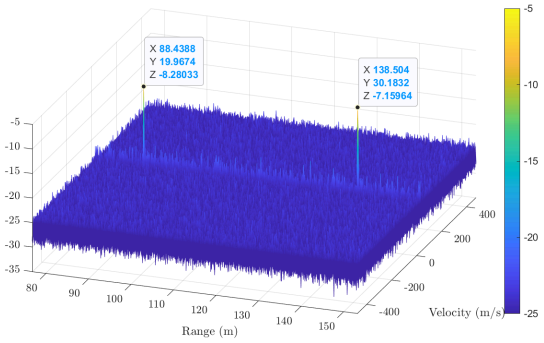

(b) RDM with adaptive FFT-based block correlator.

Fig. 6: RDM Comparison

SNR is preserved while providing processing efficiency for large sequence lengths.

Future work could explore incorporating other sensing modalities or previous RDM estimations to provide information on range sparsity to enhance the adaptive determination of the range bins of interest. Additionally, the current complexity analysis is based on individual block results; integrating block combinations into the analysis would provide an analytical framework for selecting the optimal d and b.

REFERENCES

[1] C. Waldschmidt, J. Hasch, and W. Menzel, "Automotive radar — from first efforts to future systems," *IEEE Journal of Microwaves*, vol. 1, no. 1, pp. 135–148, 2021.

[2] S. Sun, A. P. Petropulu, and H. V. Poor, "MIMO Radar for Advanced Driver-Assistance Systems and Autonomous Driving: Advantages and Challenges," *IEEE Signal Processing Magazine*, vol. 37, no. 4, pp. 98–117, 2020.

[3] D. Guermandi, Q. Shi, A. Dewilde, V. Derudder, U. Ahmad, A. Spagnolo, I. Ocket, A. Bourdoux, P. Wambacq, J. Craninckx, and W. Van Thillo, "A 79-GHz 2 × 2 MIMO PMCW Radar SoC in 28-nm CMOS," *IEEE Journal of Solid-State Circuits*, vol. 52, no. 10, pp. 2613–2626, 2017.

[4] B. Schweizer, A. Grathwohl, G. Rossi, P. Hinz, C. Knill, S. Stephany, H. J. Ng, and C. Waldschmidt, "The Fairy Tale of Simple All-Digital Radars: How to Deal With 100 Gbit/s of a Digital Millimeter-Wave MIMO Radar on an FPGA [Application Notes]," *IEEE Microwave Magazine*, vol. 22, no. 7, pp. 66–76, 2021.

[5] F. Roos, J. Bechter, C. Knill, B. Schweizer, and C. Waldschmidt, "Radar Sensors for Autonomous Driving: Modulation Schemes and Interference Mitigation," *IEEE Microwave Magazine*, vol. 20, no. 9, pp. 58–72, 2019.

[6] X. Shang, R. Lin, and Y. Cheng, "Mixed-ADC Based PMCW MIMO Radar Angle-Doppler Imaging," *IEEE Transactions on Signal Processing*, vol. 72, pp. 883–895, 2024.

[7] M. Kahlert, T. Fei, C. Tebruegge, and M. Gardill, "Stepped-Frequency PMCW Waveforms for Automotive Radar Applications," *IEEE Transactions on Radar Systems*, vol. 3, pp. 233–245, 2025.

[8] V. Oliari, W. van Houtum, and A. Pandharipande, "Reconfigurable PMCW Radar Sensor System," *IEEE Sensors Letters*, vol. 7, no. 11, pp. 1–4, 2023.

[9] M. Bauduin and A. Bourdoux, "Reducing Range Sidelobes and Ghost Targets in PMCW Radars With π/K-Zadoff Code Sequences," *IEEE Transactions on Radar Systems*, vol. 1, pp. 646–656, 2023.

[10] W. Van Thillo, P. Gioffré, V. Giannini, D. Guermandi, S. Brebels, and A. Bourdoux, "Almost perfect auto-correlation sequences for binary phase-modulated continuous wave radar," in *2013 European Radar Conference*, 2013, pp. 491–494.

[11] L. Xu and Q. Liang, "Zero Correlation Zone Sequence Pair Sets for MIMO Radar," *IEEE Transactions on Aerospace and Electronic Systems*, vol. 48, no. 3, pp. 2100–2113, 2012.

[12] T. Antes, L. G. de Oliveira, E. Bekker, A. Bhutani, and T. Zwick, "Doppler Robustness Analysis of Orthogonal Sequences for MIMO PMCW Radar," in *2022 23rd International Radar Symposium (IRS)*, 2022, pp. 384–389.

[13] C. Falsi, D. Dardari, L. Mucchi, and M. Z. Win, "Time of arrival estimation for UWB localizers in realistic environments," *EURASIP J. Adv. Signal Process*, vol. 2006, p. 152, Jan. 2006.

[14] D. Akopian and S. Agaian, "A fast time-recursive correlator for DSSS communications," *IEEE Signal Processing Letters*, vol. 15, pp. 589–592, 2008.

[15] ——, "Fast and parallel matched filters in time domain," in *Proceedings of the 17th International Technical Meeting of the Satellite Division of The Institute of Navigation (ION GNSS 2004)*, 2004, pp. 491–500.

[16] D. Akopian, P. Sagiraju, and B. Nowak, "Fast time-recursive block correlators for pseudorandom sequences," *IEEE Transactions on Circuits and Systems I: Regular Papers*, vol. 60, no. 7, pp. 1835–1844, 2013.

[17] J. Leclère, C. Botteron, R. Landry, and P.-A. Farine, "FFT Splitting for Improved FPGA-Based Acquisition of GNSS Signals," *International Journal of Navigation and Observation*, vol. 2015, pp. 1–12, 2015.

[18] J. Leclère, "Resource-efficient parallel acquisition architectures for modernized gnss signals," EPFL, Tech. Rep., 2014.

[19] J. Leclère, C. Botteron, and P.-A. Farine, "Acquisition of modern GNSS signals using a modified parallel code-phase search architecture," *Signal Processing*, vol. 95, pp. 177–191, 2014.

[20] R. G. Lyons, *Understanding Digital Signal Processing*, 3rd ed. Prentice Hall, 2010.